The International Archives of the Photogrammetry, Remote Sensing and Spatial Information Sciences, Volume XLVI-4/W3-2021
Joint International Conference Geospatial Asia-Europe 2021 and GeoAdvances 2021, 5–6 October 2021, online

ASSESSMENT OF URBAN ENVIRONMENTAL QUALITY: A CASE STUDY OF CASABLANCA, MOROCCO

A. Malah[1]*, H. Bahi[1], H. Radoine[1], M. Maanan[2], H. Mastouri[1]

[1] School of Architecture, Planning & Design, Mohammed VI Polytechnic University, Benguerir, Morocco – anass.malah@um6p.ma
[2] Earth Sciences Department, Faculty of Sciences Ain Chock, Hassan II University of Casablanca, Casablanca, Morocco

Commission 4, WG 7

KEY WORDS: Urban Environmental quality, Remote sensing, GIS, Principal components analysis, Casablanca

ABSTRACT

By 2050, Most of the world's population will live in cities, this demographic explosion will lead to significant urban development at the expanse of natural land which may harm the environmental quality. Consequently, assessing and modeling the urban environmental quality (UEQ) is requisite for efficient urban sprawl control and better city planning and management. The present study proposes a methodology to model and assess the environment of the urban system by developing the urban environmental quality index (UEQI) based on remote sensing data. Five environmental indicators were derived from the Landsat OLI image namely, Modified Normalized Difference Impervious Surface Index (MNDISI), Modified Normalized Difference, Water Index (MNDWI), Normalized difference vegetation Index (NDVI), Normalized difference built-up Index (NDBI) and Soil adjusted vegetation index (SAVI). Using the Principal Component Analysis (PCA) the urban environmental quality index was computed for the 17 communes of Casablanca city. The UEQI values were spatially mapped under three classes (good, moderate, and poor). The results obtained from the analysis showed a significant difference in the term of UEQI values among the communes. In addition, the environmental quality is inadequate in communes with fewer green spaces and more impervious surfaces. The outcomes of this work can serve as an efficient tool to determine the most critical interventions to be made by the authority for current and future urban planning and land/resource management.

1. INTRODUCTION

The Urbanization is one of the most serious challenges and critical processes (Bettencourt & West, 2010; Chadchan & Shankar, 2009). In 2018, 55.3 percent of the world's population lived in urban areas, a proportion that is expected to increase to 60 percent by 2030 (United Nations, Department of Economic and Social Affairs, 2018). Currently, over 50 percent of the population lives in urban areas in Africa. In Morocco, 60 percent of the population resides in urban areas, as opposed to 35 percent in 1970 and by 2050, nearly three-quarters of the population will be living in cities (Lall et al., 2019).

This urban revolution has induced great effects on the socio-economic sustainability of communities and serious environmental problems (Luan & Li, 2021; Yuan, 2008) including the increases in impervious surfaces, energy demands, urban heat islands, water and air pollution, the treatment of solid waste, and the loss of natural vegetation, open spaces and wildlife habitat (Ann et al., 2008; Bahi et al., 2016; Cao et al., 2016; Forman & Wu, 2016; Santana et al., 2018; Senanayake et al., 2013). Thus, the city authorities and planners will need to incorporate new policies that endorse sustainable development and smart growth in anticipation of the urban disadvantages to improve urban environmental quality.

Urban environmental quality is a complex and variable parameter that is used to describe the interaction that exists between different factors which are positively or negatively impact the quality of the environment (Elariane et al., 2013; Faisal & Shaker, 2017). It is challenging to model and predict the interaction of diverse factors because these variables have different units. Recently, remotely sensed imagery is an effective data source for modeling urban environmental quality (UEQ) because the imagery can provide continuous Earth observation images of the urban environment at different spatial, spectral, and temporal resolutions (Du et al., 2014; Javanbakht et al., 2021). Assessing the UEQ is an effective tool in urban planning and management since it provides more specific information about urban conditions, it may also be a powerful tool for informing the public about the quality of the environment in which they live. In this research, we focused on the assessment of urban environmental quality using environmental variables obtained from remote sensing imagery by developing a new synthetic index.

2. STUDY AREA

In this research, the city of Casablanca has been selected as the study area (Figure 1). It is located in the center-west of Morocco on the Atlantic coast, about 80 Km south of the Moroccan administrative capital (Rabat). Spread on the Atlantic coast for nearly 14 Km, Casablanca is influenced by moderate air temperatures compared to other Moroccan and subtropical cities (Zerhouny et al., 2018). Casablanca is the main economic, financial, and urban center of the country and it is the largest city in Morocco with an area of 386.14 Km², it contains nearly 12.6% of the Moroccan population (High Commissioner for Planning, 2014). In terms of demographic evolution, the city of Casablanca is considered the most dynamic city in Morocco. From an administrative prospect, the city includes 17 communes and each commune has been identified by an ID to assist the representation of the study area.

https://doi.org/10.5194/isprs-archives-XLVI-4-W3-2021-205-2022 |

3. MATERIAL AND METHODS

In this research the overall methodology followed is represented in Figure 2. For our work, two data sources were used: 1) Vector map of commune limits, provided by the urban agency of Casablanca, For the municipality administration, the city is divided into 17 communes, which are identified by the numbers 1–17. Table 1 represents the 5 factors used in this study. Landsat 8 satellite imagery, by the United States Geological Survey (USGS). 2). Landsat 8 satellite imagery, by the United States Geological Survey (USGS).

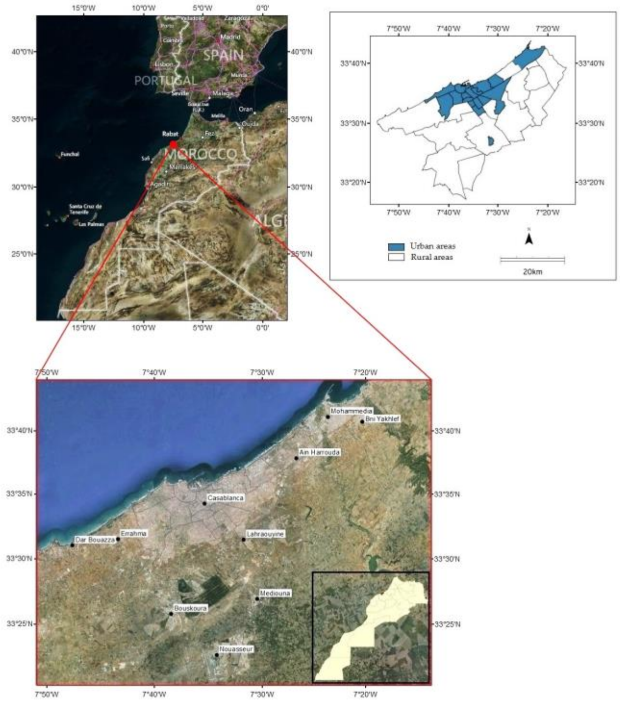

Figure 1. Location of the study area. (Bahi et al., 2016).

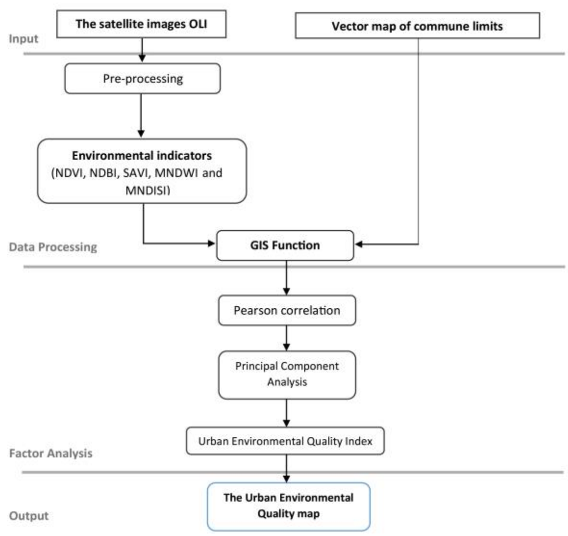

Figure 2. Flowchart representing the research design process.

The radiometric calibration was performed for the Landsat 8 image by converting the digital numbers to the top of atmosphere spectral radiance and reflectance (Bahi et al., 2016; Czapla-Myers et al., 2015). In the view of the equations listed in Table 1, the five environmental indicators Modified Normalized Difference Impervious Surface Index (MNDISI) Modified Normalized Difference Water Index (MNDWI) Normalized difference vegetation index (NDVI) Normalized difference built-up Index (NDBI) Soil adjusted vegetation index (SAVI) were attained based on the Python programming language with the GDAL libraries and NumPy (Guha et al., 2021; Huete, 1988; Santana et al., 2018; Wang et al., 2017; Xu, 2007). The mean values at the commune level of each indicator were calculated using the spatial statistics function based on the vector map of commune limits.

Based on the Principal Component Analysis (PCA) the weights were derived for the five environmental factors. Before running PCA, The Kaiser Meyer Olkin (KMO), Bartlett's test, and the communality of variables were performed to evaluate the suitability of the data for the PCA (Iwaniak et al., 2018; Joseph et al., 2014). The retained component had an eigenvalue of more than 1, this component describes the maximum of the total variance (Du et al., 2014). The weights of the indicators on the retained component were used in the interpretation and to develop a new synthetic index using the percentage of variance (Krishnan & Firoz, 2020).

Environmental Indicators	Formula
MNDISI	= [TS − (MNDWI + NIR + SWIR1)/3] / [TS + (MNDWI + NIR + SWIR1)/3]
MNDWI	= (Green - SWIR1) / (Green + SWIR1)
NDVI	= (NIR - RED) / (NIR + RED)
NDBI	= (SWIR - NIR) / (SWIR + NIR)
SAVI	= [(NIR - RED) / (NIR + RED + L)] * (1 + L)

Table 1. The five environmental indicators used to assess UEQI, Modified Normalized Difference Impervious Surface Index (MNDISI). Normalized difference built-up index (NDBI). Soil Adjusted Vegetation Index (SAVI). Normalized Difference Vegetation Index (NDVI). Modified Normalized Difference Water Index (MNDWI).

4. RESULTS AND DISCUSSIONS

4.1 Environmental variables

In this study, 5 environmental variables were selected to derive the synthetic index of urban environment quality. Regarding these indicators, the impervious surfaces and NDBI are high, while the green spaces are less, as indicate by the NDVI and SAVI. It can easily be seen in figure 3 the lowest value of NDVI and the highest value of the impervious surfaces and NDBI at the North and East parts of the city, in the zone of the Casablanca port (commune 10), and in the industrial areas of the city (commune 3, 11 and 12) the same case for the communes 1, 2 and 5 in the downtown. However, the values of NDVI are high in the eastern part of the city in parks and villa zones (commune 9 and 15).

The Pearson correlation was calculated to give a preliminary analysis of the relationships among the 5 indicators. Table 2 represents the correlation matrix. The MNDISI and NDBI have a strong positive correlation, also there is a high to moderate positive correlation among NDVI and SAVI, and MNDWI while they are negatively correlated with MNDISI and NDBI.

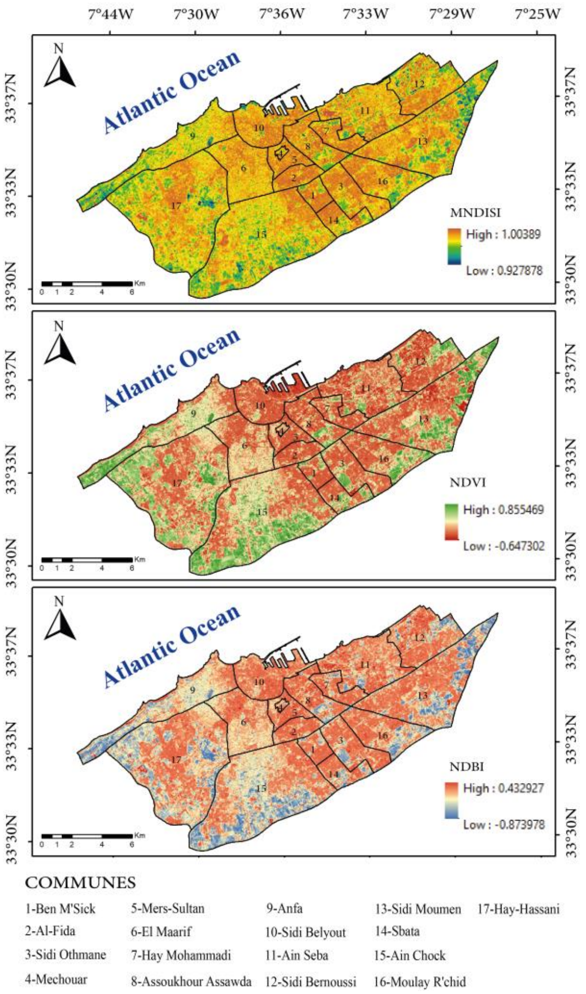

Figure 3. MNDISI NDVI and NDBI.

	MNDISI	NDBI	SAVI	NDVI	MNDWI
MNDISI	1	.921**	-.833**	-.813**	-.663**
NDBI	.921**	1	-.972**	-.967**	-,440
SAVI	-.833**	-.972**	1	.998**	,218
NDVI	-.813**	-.967**	.998**	1	,205
MNDWI	-.663**	-,440	,218	,205	1

Modified Normalized Difference Impervious Surface Index (MNDISI). Normalized difference built-up index (NDBI). Soil Adjusted Vegetation Index (SAVI). Normalized Difference Vegetation Index (NDVI). Modified Normalized Difference Water Index (MNDWI).
**. Correlation is significant at the 0.01 level (2-tailed).
*. Correlation is significant at the 0.05 level (2-tailed).

Table 2. The Pearson correlation matrix.

4.2 Principal component analysis and UEQI

As mentioned above, the five environmental indicators were derived using remote sensing and calculating the mean value of each environmental indicator per commune. In order to combine the five indicators into a single index the PCA was used as weighting technique. To assess the suitability of these indicators for the principal component analysis the Kaiser Meyer Olkin (KMO), Bartlett's test was used (Table 3). The data can be acceptable for PCA if the KMO is more than 0.5 and the significant level of Bartlett's test is less than 0.1 (Liang & Weng, 2011). The result of KMO was 0.617 and the significant level of Bartlett's Sphericity was 0.000, which confirmed the suitability of principal component analysis application for our study.

Based on the correlation matrix, the principal component analysis produced one component with an eigenvalue more than 1 by using the Kaiser criteria (Schreiber, 2021). According to (Iwaniak et al., 2018) the number of PCs may be described by cumulative variance, exceeding a threshold value depending on the specificity of data analyzed. Usually, the sufficient threshold value of cumulative variance is at least 70% and in some cases 80%. In our study, the retained component represented 79.028 % of the variance (Table 4).

KMO		**,617**
Bartlett's Test of Sphericity	Approximate $\chi 2$	217,091
	Degrees of freedom	10
	Significance	**,000**

Table 3. Results of the KMO and Bartlett´s test.

Variable	Component
NDBI	-,996
SAVI	,953
MNDISI	-,953
NDVI	,946
MNDWI	,499
Eigenvalue	3,951
Variance (%)	79,028

Table 4. Rotated component matrix.

Table 4 shows the component loadings for each indicator after rotation. This component has strong positive loadings (Correlation) with NDVI and SAVI variables indices to vegetation and very strong negative loadings with NDBI and MNDISI variables linked to impervious surfaces vegetation. This component increases with rising of green areas and decreases with the existence of impervious surfaces (buildings, roads, parking lot…). The larger score of the component indicates better environmental quality.

This contribution has been peer-reviewed.
https://doi.org/10.5194/isprs-archives-XLVI-4-W3-2021-205-2022

Communes	ID	Scores	UEQI
Ben M'Sick	1	-0,68	-0,53
Al-Fida	2	-1,34	-1,06
Sidi Othmane	3	-0,49	-0,39
Mechouar	4	-0,27	-0,21
Mers-Sultan	5	-1,28	-1,01
El Maarif	6	0,03	0,02
Hay Mohammadi	7	-0,82	-0,65
Assoukhour Assawda	8	-0,38	-0,30
Anfa	9	2,21	1,75
Sidi Belyout	10	-0,90	-0,71
Ain Seba	11	-0,32	-0,25
Sidi Bernoussi	12	0,04	0,03
Sidi Moumen	13	0,92	0,72
Sbata	14	0,08	0,06
Ain Chock	15	1,75	1,38
Moulay R'chid	16	0,41	0,32
Hay-Hassani	17	1,04	0,82

Table 5. Component scores for communes.

The urban environmental quality index was created using the model presented below. In addition to the component score for each commune (Table 5), some authors (Du et al., 2014; Krishnan & Firoz, 2020; Santana et al., 2018) recommend using the percentage of variance obtained in the analysis as a component weight (1).

(1)

UEQI = (variance explains by component *component score) /100

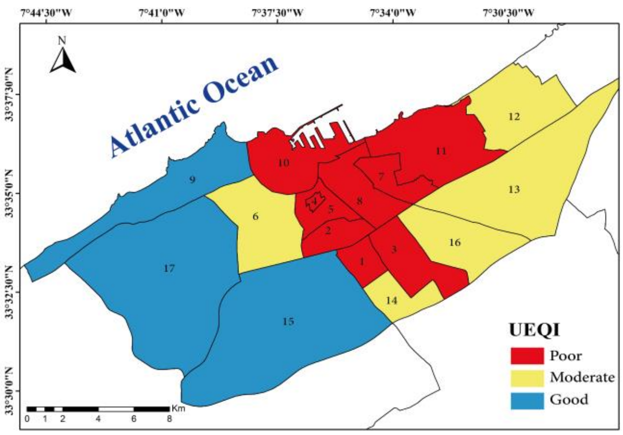

Figure 4. The Urban Environment Quality Index of the 17 communes of Casablanca city.

The result of the urban environmental quality index per commune is presented in Figure 4. The UEQI was normalized between 0 and 1 first. To represent the choropleth map of the UEQI, some authors (De Deus et al., 2013; Krishnan & Firoz, 2020; Nelson et al., 2015; Santana et al., 2018; Shao et al., 2016; Zou & Yoshino, 2017) recommend using equal intervals to assist in the interpretation of the results. To express the urban environmental quality three classes were chosen: poor (UEQI values between 0 – 0.33), moderate (0.34 – 0.67), and good (0.68 – 1). The spatial distribution of the urban environmental quality index shows that the poor class is corresponding to communes located in the central and the North (communes 1, 2, 3, 4, 5, 7, 8, 10, 11, and 12), these communes considered as the most crowded areas as they have the highest housing and population density in Casablanca between 424 and 350 inhabitants per hectare, with the existence of the industrial zones (communes 8, 10 and 11) and commercial areas (communes 5 and 7). In contrast, the impervious surfaces are low in the West side of the city in parks and villa zones at the communes 9, 15, and 17, these communes are classed as good which have low housing density less than 115 inhabitants per hectare and larger green spaces, particularly commune 9, this commune has a very good urban design (parks and villa zones), and a high socioeconomic level.

5. CONCLUSION

In summary, this research has presented a methodology to assess the Urban Environmental Quality (UEQ) at commune level in Casablanca city, based on the integration of five environmental indicators derived from remote sensing. Since UEQ is a multidisciplinary and complex subject, there are numerous methods to assess the environmental quality in urban areas. This study gives a methodological approach, to interpret the relationships between different environmental indicators through the spatial distribution of the urban environmental quality index. The results showed that the environment quality is inadequate in more than half of the study area communes which constitute only 25% of the urban territory. In contrast, only 3 communes have good environmental quality, these communes represent more than 44% of the urban areas, which indicates that the urban design is an essential factor in the urban environmental quality. The method introduced in this work can replicate for cities with similar conditions, which provides important information for urban planners for better urban planning and management.

REFERENCES

Ann, K., Jago-on, B., Kaneko, S., Fujikura, R., Fujiwara, A., Imai, T., Matsumoto, T., Zhang, J., Tanikawa, H., & Tanaka, K. (2008). Urbanization and subsurface environmental issues : An attempt at DPSIR model application in Asian cities. *Science of the Total Environment, The*, *407*(9), 3089–3104. https://doi.org/10.1016/j.scitotenv.2008.08.004

Bahi, H., Rhinane, H., Bensalmia, A., Fehrenbach, U., & Scherer, D. (2016). Effects of urbanization and seasonal cycle on the surface urban heat island patterns in the coastal growing cities: A case study of Casablanca, Morocco. *Remote Sensing*, *8*(10). https://doi.org/10.3390/rs8100829

Bettencourt, L., & West, G. (2010). A unified theory of urban living. *Nature*, *467*(7318), 912–913. https://doi.org/10.1038/467912a

Cao, C., Lee, X., Liu, S., Schultz, N., Xiao, W., Zhang, M., & Zhao, L. (2016). Urban heat islands in China enhanced by haze pollution. *Nature Communications*, *7*, 1–7. https://doi.org/10.1038/ncomms12509

Chadchan, J., & Shankar, R. (2009). Emerging urban development issues in the context of globalization. *Journal of ITPI (Institute of Town Planners India), 6(2)*(April 2009), 78–85.

Czapla-Myers, J., McCorkel, J., Anderson, N., Thome, K., Biggar, S., Helder, D., Aaron, D., Leigh, L., & Mishra, N. (2015). The ground-based absolute radiometric calibration of Landsat 8 OLI. *Remote Sensing*, *7*(1), 600–626. https://doi.org/10.3390/rs70100600

De Deus, L. R., Garcia Fonseca, L. M., & De Marcelhas E Souza, I. (2013). Creating an socio-environmental condition index to assess of urban environmental quality. *Joint Urban Remote Sensing Event 2013, JURSE 2013*, *856*(1), 271–274. https://doi.org/10.1109/JURSE#.2013.6550717

Du, P., Liu, P., Xia, J., Feng, L., Liu, S., Tan, K., & Cheng, L. (2014). Remote sensing image interpretation for urban environment analysis: Methods, system and examples. *Remote Sensing*, *6*(10), 9458–9474. https://doi.org/10.3390/rs6109458

Elariane, S. A., Serag El Din, H., Shalaby, A., & Farouh, H. E. (2013). Principles of urban quality of life for a neighborhood. *HBRC Journal*, *9*(1), 86–92. https://doi.org/10.1016/j.hbrcj.2013.02.007

Faisal, K., & Shaker, A. (2017). An investigation of GIS overlay and PCA techniques for urban environmental quality assessment: A case study in Toronto, Ontario, Canada. *Sustainability (Switzerland)*, *9*(3), 1–25. https://doi.org/10.3390/su9030380

Forman, R. T. T., & Wu, J. (2016). Where to put the next billion people. *Nature*, *537*(7622), 608–611. https://doi.org/10.1038/537608a

Guha, S., Govil, H., Gill, N., & Dey, A. (2021). A long-term seasonal analysis on the relationship between LST and NDBI using Landsat data. *Quaternary International*, *575–576*(July), 249–258. https://doi.org/10.1016/j.quaint.2020.06.041

High Commissioner for Planning. (2014). *General Census of Population and Housing 2014. Presentation Note of the Results Greater Casablanca Region*. https://www.hcp.ma/reg-casablanca/RGPH-2014_r5.html

Huete, A. R. (1988). A Soil-Adjusted Vegetation Index (SAVI). *Remote Sensing of Environment*, *15*(1), 295–309.

Iwaniak, A., Hrynkiewicz, M., Bucholska, J., Darewicz, M., & Minkiewicz, P. (2018). Structural characteristics of food protein-originating di- and tripeptides using principal component analysis. *European Food Research and Technology*, *244*(10), 1751–1758. https://doi.org/10.1007/s00217-018-3087-3

Javanbakht, M., Darvishi Boloorani, A., Kiavarz, M., Neisany Samany, N., Zebardast, L., & Zangiabadi, M. (2021). Spatial-temporal analysis of urban environmental quality of Tehran, Iran. *Ecological Indicators*, *120*(August 2020), 106901. https://doi.org/10.1016/j.ecolind.2020.106901

Joseph, M., Wang, F., & Wang, L. (2014). GIS-based assessment of urban environmental quality in Port-au-Prince, Haiti. *Habitat International*, *41*, 33–40. https://doi.org/10.1016/j.habitatint.2013.06.009

Krishnan, S., & Firoz, M. (2020). *Regional urban environmental quality assessment and spatial analysis*. https://doi.org/10.1016/j.jum.2020.03.001

Lall, S., Mahgoub, A., Maria, A., Touati, A., & Acero, J. L. (2019). *Leveraging Urbanization to Promote a New Growth Model While Reducing Territorial Disparities in Morocco*. https://openknowledge.worldbank.org/bitstream/handle/10986/31877/9781464814334.pdf?sequence=2

Liang, B., & Weng, Q. (2011). Assessing urban environmental quality change of indianapolis, united states, by the remote sensing and GIS integration BT - SPECIAL ISSUE ON HUMAN SETTLEMENTS: A GLOBAL REMOTE SENSING CHALLENGE and SPECIAL ISSUE ON EARTH OBSERVATIONS AND REMOTE SENSING F. *IEEE Journal of Selected Topics in Applied Earth Observations and Remote Sensing*, *4*(1), 43–55. https://doi.org/10.1109/JSTARS.2010.2060316

Luan, W., & Li, X. (2021). Rapid urbanization and its driving mechanism in the Pan-Third Pole region. *Science of the Total Environment*, *750*, 141270. https://doi.org/10.1016/j.scitotenv.2020.141270

Nelson, J. R., Grubesic, T. H., Sim, L., Rose, K., & Graham, J. (2015). Approach for assessing coastal vulnerability to oil spills for prevention and readiness using GIS and the Blowout and Spill Occurrence Model. *Ocean & Coastal Management*, *112*, 1–11. https://doi.org/10.1016/J.OCECOAMAN.2015.04.014

Santana, L. M., Barona, D. A., & Musse, M. A. (2018). Urban environmental quality assessment using remote sensing and census data. *International Journal of Applied Earth Observation and Geoinformation*, *71*(October 2017), 95–108. https://doi.org/10.1016/j.jag.2018.05.010

Schreiber, J. B. (2021). Issues and recommendations for exploratory factor analysis and principal component analysis. *Research in Social and Administrative Pharmacy*, *17*(5), 1004–1011. https://doi.org/10.1016/j.sapharm.2020.07.027

Senanayake, I. P., Welivitiya, W. D. D. P., & Nadeeka, P. M. (2013). Remote sensing based analysis of urban heat islands with vegetation cover in Colombo city, Sri Lanka using Landsat-7 ETM+ data. *Urban Climate*, *5*, 19–35. https://doi.org/10.1016/j.uclim.2013.07.004

Shao, H., Sun, X., Wang, H., Zhang, X., Xiang, Z., Tan, R., Chen, X., Xian, W., & Qi, J. (2016). A method to the impact assessment of the returning grazing land to grassland project on regional eco-environmental vulnerability. *Environmental Impact Assessment Review*, *56*(2016), 155–167. https://doi.org/10.1016/j.eiar.2015.10.006

United Nations, Department of Economic and Social Affairs, P. D. (2018). The World 's Cities in 2018. *The World's Cities in 2018 - Data Booklet (ST/ESA/ SER.A/417)*, 34.

Wang, C., Sun, Z., Guo, H., & Shang, R. (2017). A modified normalized difference impervious surface index (MNDISI) for automatic urban mapping from landsat imagery. *Remote Sensing*, *9*(9), 1–18. https://doi.org/10.3390/rs9090942

Xu, H. (2007). Modification of normalised difference water index (NDWI) to enhance open water features in remotely sensed imagery. *International Journal of Remote Sensing*, *27*(14), 3025–3033. https://doi.org/10.1080/01431160600589179

Yuan, F. (2008). International Journal of Remote. *International*

Journal of Remote Sensing, 768515118. https://doi.org/10.1080/01431160701294703

Zerhouny, M., Fadil, A., & Hakdaoui, M. (2018). Underground space utilization in the urban land-use planning of Casablanca (Morocco). *Land*, *7*(4). https://doi.org/10.3390/land7040143

Zou, T., & Yoshino, K. (2017). Environmental vulnerability evaluation using a spatial principal components approach in the Daxing'anling region, China. *Ecological Indicators*, *78*, 405–415. https://doi.org/10.1016/j.ecolind.2017.03.039